Effect of thermal annealing on the dielectric, passivation and pH detection properties of aluminium oxide thin films deposited by plasma-enhanced atomic layer deposition

Ahmet Lale, Matthieu Joly, Samir Mekkaoui, Xavier Joly, Emmanuel Scheid, Jérôme Launay, Pierre Temple-Boyer

Effect of thermal annealing on the dielectric, passivation and pH detection properties of aluminium oxide thin films deposited by plasma-enhanced atomic layer deposition

A. Lale[1,2], M. Joly[1,2], S. Mekkaoui[1,2], X. Joly[1,2], E. Scheid[1,2], J. Launay[1,2], Pierre Temple-Boyer[1,2]

[1] CNRS, LAAS, 7 avenue du colonel Roche, F-31400 Toulouse, France

[2] Université de Toulouse, UPS, LAAS, F-31400 Toulouse, France

Abstract:

The dielectric properties of aluminium oxide (Al_2O_3) thin films obtained by plasma-enhanced atomic layer deposition (PEALD) from $Al(CH_3)_3/O_2$ precursors were investigated while focusing on the influences of thermal annealing under a dioxygen (O_2) ambient. PEALD-Al_2O_3-based metal-insulator-silicon structures/capacitors and pH-sensitive chemical field effect transistors were fabricated to deal respectively with microelectronic applications and measurement in liquid phase. Antagonist results were thus evidenced. On the one hand, dealing with high-k gate materials, optimized dielectric properties, i.e. low fixed charge density (4×10^{12} cm^{-2}), high dielectric constant ($\varepsilon_r = 10.2$), Fowler-Nordheim conduction and high breakdown electric fields ($E_{bd} = 8.75$ MV/cm) were obtained for polycrystalline PEALD Al_2O_3 films annealed at high temperature (T > 750°C). On the other hand, pH detection properties, i.e. quasi-Nernstian sensitivity (59 mV/pH), low drift (< 1 mV/day) and long lifetime (> 180 days), were optimized for unannealed amorphous PEALD Al_2O_3 films. These phenomena were associated germination/crystallization phenomena in the deposited amorphous alumina structure as well as to related charge trapping and leakage currents in water-based solutions related to the final Al_2O_3 polycrystalline structure.

Keywords: Plasma-enhanced atomic layer deposition, Aluminium oxide, Thermal annealing, Dielectric properties, pH measurement, Field-effect transistor-based devices

1. Introduction

In the frame of microtechnologies, aluminium oxide (Al_2O_3) thin films were integrated while using many different processes based on physical and/or chemical techniques: evaporation, sputtering, laser deposition and of course chemical vapour deposition [1-6]. Among them, atomic layer deposition (ALD) was thoroughly studied, emphasizing the use of trimethylaluminium $Al(CH_3)_3$ (TMA) and dioxygen (O_2) based plasma as aluminium and oxygen sources respectively [7-12]. Nevertheless, if alumina thin films were studied in the frame of numerous applications, their insulative properties were usually highlighted, either as a "high-k" (high dielectric constant) gate material for metal-oxide-silicon (MOS) microdevices [13-14], either as passivation insulative layer for field-effect-based chemical nanosensors [15-20]. Indeed, as an insulator, Al_2O_3 is characterized by a large bandgap (~ 9 eV) and therefore high breakdown electric field, high dielectric permittivity ($\varepsilon_r \approx 9$) as well as high resistivity and therefore low leakage currents, good adhesion and interfacial properties with silicon-based layers and thus low interface trap densities, and finally excellent chemical and thermal stabilities below the crystallization temperature (750-800°C) [21]. Consequently, whatever the deposition process used, specific attentions were brought on the study of alumina thin films dielectric properties thanks to the realisation of Metal-Insulator-Silicon or Metal–insulator–Metal integrated capacitors [6,21-28]. However, in the frame of pH-sensitive electrochemical sensors, even if Al_2O_3-based gate sensitive layers were proposed [29-30] for pH-ChemFET (pH-sensitive chemical field effect transistor) microdevices and further improved for associated nanodevices [15-20], main focuses were brought on other metal-oxide-based materials: Ta_2O_5, TiO_2, RuO_2, IrO_2,… [31]. As a result, still dealing with alumina Al_2O_3 films, optimizations and compromises have to be found according to their deposition processes.

In this context, this paper proposes to investigate the dielectric and passivation properties of alumina thin films obtained by plasma-enhanced atomic layer deposition (PEALD) from $Al(CH_3)_3/O_2$ precursors, focusing on the influence of thermal annealing while taking into account the final application: microelectronics or pH potentiometric detection in water-based solutions.

2. Experimental details

Growth experiments were carried out in a FIJI F200 plasma-enhanced atomic layer deposition (PEALD) equipment developed by CAMBRIDGE NANOTECH company. Al_2O_3 films were deposited using conventional experimental conditions (deposition temperature: 300°C, base pressure: ~ 9.3 Pa) from trimethylaluminium $Al(CH_3)_3$ (TMA) and dioxygen (O_2). A standard cyclic routine was chosen to saturate the growth rate while preventing any undesirable gaseous mixing: TMA injection in gaseous phase (duration: 0.025 s), purge (argon: 180 sccm, duration: 6 s), plasma O_2 exposure (O_2: 20 sccm, plasma power: 300 W, duration: 20 s), purge (argon: 180 sccm, duration: 6 s) [8,12,32]. As a result, each PEALD deposition process were defined by its number of TMA/O_2 PEALD cycles. Finally, during the different fabrication processes, alumina layers and associated device wafers (see hereafter) were annealed at atmospheric pressure under a dioxygen (O_2) ambient (duration: 5 minutes) using an ANNEALSYS AS-Master-2000HT rapid thermal process (RTP) equipment.

Alumina films were studied by spectroscopic ellipsometry using an UVISEL equipment from HORIBA JOBIN YVON while working at a 450 nm wavelength (accuracy measurement: ± 2%). Thus, thicknesses of the different deposited and/or annealed films were estimated while considering $SiO_2/Al_xSi_yO/Al_2O_3$ non-conventional structures [12]. Dielectric properties of PEALD Al_2O_3 films were finally studied while according to different capacitive structures. Firstly, a "400 cycle" alumina film (estimated thickness: 38 ± 1 nm) was deposited by PEALD on (100)-oriented, p-type

(10-12 Ω.cm) silicon substrates and metal-insulator-silicon (MIS) structures were obtained thanks to the use of a mercury-based capacitive probe (MDC company, model 802C, mercury contact area: 4.18×10^{-3} cm^2) and an AGILENT 4294A analyser. The accuracy of the whole technique was estimated at $\pm$ 5%.

Secondly, PEALD-Al$_2$O$_3$-based MIS capacitors were fabricated on (100)-oriented, p-type (10-12 Ω.cm) silicon substrates using a conventional "Thick field oxide" process [33]. First, an 800 nm thick oxide was grown thermally in a wet (H$_2$/O$_2$ ratio: 1.8) ambient at high temperature (1070°C). Then, photolithography and BHF (buffered hydrofluoric acid) chemical etching was used to define capacitors with areas ranging from 1.6×10^{-6} to 7.84×10^{-2} cm^2 in order to study both dielectric and conduction properties. After an appropriated cleaning, a "325 cycle" alumina film was deposited by PEALD (thickness: 30 $\pm$1 nm) to form the gate insulative layer. Finally, electrical contacts were formed by evaporation of aluminum (thickness: 200 nm). On the front side of the silicon substrate, photolithography and chemical etching were performed according to a specific photolithographic pattern adapted to statistic probe testing. On its back side, metallization covered the whole substrate surface to ensure a good electrical contact with the probe test chuck. Ellipsometric test patterns (area: $5 \times 5\ 10^{-2}$ mm$^{2)}$) were realized during the MIS fabrication process in order to check the PEALD-Al$_2$O$_3$ film thickness (accuracy measurement: $\pm$ 2%).

Thirdly, front-side connected, pH-sensitive chemical field effect transistors were fabricated on (100)-oriented, n-type silicon substrates according to a well-known "P-well technology" process [34]. Thus, a 50 nm thermally grown SiO$_2$ layer and a 50 nm PEALD Al$_2$O$_3$ layer (number of cycles: 550) deposited on top formed the pH-sensitive gate structure. This cycle number and associated thickness were chosen specifically in order to fit with standard SiO$_2$ (50nm)/Si$_3$N$_4$ (50nm) pH-ChemFET microdevices also realized for comparison.

For all the different MIS structures studied, capacitance – voltage (C-V) experiments were performed on thin PEALD Al$_2$O$_3$ films at 1, 10, 100 and 1000 kHz (potential range: [-10 V, +10 V],

sinusoidal signal: 100 mV) using an AGILENT 4294A impedance analyser. Finally, current–voltage (I-V) analyses were performed statistically using an AGILENT 4142B analyser coupled with a KARLSUSS Pa200 probe station.

pH-ChemFET microdevices were characterized by current – voltage (I-V) measurements in buffered solutions (pH = 4.0, 7.0 and 10.0) using an AGILENT 4142B analyser. In parallel, titration experiments using hydrochloric acid (HCl: 10^{-2} M) and tetra-methyl-ammonium hydroxide (TMAH: 10^{-1} M) were performed to study pH detection properties. In this context, a specific "source-drain follower" measurement interface was used. It was used to monitor continuously the gate-source voltage V_{GS} of the pH-ChemFET microsensors while working in saturation mode thanks to constant drain-source voltage V_{DS} and drain-source current I_{DS} (typically V_{DS} = 2 V and I_{DS} = 0.1 mA). Furthermore, a commercial reference electrode (METROHM Ag/AgCl glass double junction) was used to bias the analysed solution to the mass (V_G = 0).

3. Results and discussion

3.1. Dielectric properties of PEALD-Al$_2$O$_3$ thin films

In order to overview rapidly the influences of thermal annealing on the dielectric properties of PEALD alumina films, initial C-V experiments were performed on the standard "400 cycle" Si/Al$_2$O$_3$ structure (thickness: 38 ± 1 nm) while using the mercury-based capacitive probe (contact area: 4.18×10^{-3} cm^2). So, the as-deposited structure exhibit degraded C-V curves compared to the "annealed" ones (figures 1a and 1b). Indeed, if no hysteresis was found in both cases, as-deposited films show a shoulder corresponding to interface states at the Al$_2$O$_3$/Si interface [21] (figure 1a). This phenomenon should be related to the presence of an Al$_x$Si$_y$O aluminosilicate underlayer in as-deposited films [12]. Since annealing at temperature higher than 600°C was found to be responsible for the break out of this Al$_x$Si$_y$O aluminosilicate underlayer, it should also be associated to the

5

improvement of the interface between the alumina film and the silicon substrate. Consequently, no interface states and therefore optimal C-V curves were evidenced for the PEALD-Al_2O_3 films annealed at temperature higher than 750°C (as seen at 850°C, figure 1b).

Then, C-V data were studied using a fit program to determine the capacitive structure main characteristics. Data were then analysed thanks to planar capacitor equations while assuming that the dielectric constant of the SiO_2-based underlayer is equal to 4 (table 1). As expected, the "400 cycle" PEALD film was characterized by a thickness of 37 nanometres, associated to a bilayer structure formed from aluminosilicate Al_xSi_yO (5 nm) and alumina Al_2O_3 (32 nm) [12]. Then, O_2 annealing was responsible for thermal diffusion and rearrangement of oxygen, aluminium and silicon atoms in order to form an equivalent SiO_2 (4 nm)/Al_2O_3 (31 nm) structure with a total thickness of 35 nanometres.

Simultaneously, the annealing temperature increase was associated with a sigmoidal increase of the Al_2O_3 layer dielectric constant [12], as well as with a linear decrease of the fixed charge density (table 1). In order to explain these results, two phenomena have to be considered. At low temperature (T < 750°C), the annealing process is only responsible for atomic rearrangements into the Al-Si-O structure and, consequently, for the transformation of the initial $Si/Al_xSi_yO/Al_2O_3$ structure to the final $Si/SiO_2/Al_2O_3$ one [12]. Such phenomenon has no influence on the dielectric constant value but implies a decrease of the fixed charge density.

Then, as shown by X-ray diffraction (XRD) experiments in previous works [12], alumina crystallization occurs for temperature higher than 750°C. This phenomenon is responsible for the increase of the Al_2O_3 dielectric constant from 8.5 towards 10.2 (in agreement with standard values obtained for bulk monocrystalline alumina or sapphire [35]). In parallel, the fixed charge density continues to decrease towards minimal value around 4×10^{12} cm^{-2}, as already shown in literature [21]. Finally, at 900°C and more, polycrystalline alumina is definitively obtained and no further improvement of dielectric properties was evidenced.

As a matter of fact, if "high-k" gate materials for metal-oxide-silicon (MOS) microdevices are considered, the dielectric properties of PEALD Al_2O_3 films is clearly improved while using an optimized (typically 5 minutes under a dioxygen O_2 atmospheric ambient at 900°C) crystallisation annealing.

3.2. Dielectric characteristics of PEALD-Al₂O₃-based MIS capacitors

According to previous results (see below), two process conditions were tested for the microfabrication of PEALD-Al_2O_3-based Metal-Insulator-Silicon capacitors: "as-deposited" and "annealed at 900°C". C-V characterizations were performed on the largest MIS capacitors (area: 7.84×10^{-2} cm^2) to improve capacitance measurement accuracy. As previously, data were analysed using a fit program based on planar capacitor equations. C-V results obtained for Al/Al_2O_3/Si structures confirmed the previous one (figure 2a and 2b). "As-deposited" PEALD amorphous alumina films were characterized by low dielectric constant ($\varepsilon_r = 8.5$) and higher fixed charge density ($N_{ss} = 6.6 \times 10^{12}$ cm^{-2}) whereas "annealed at 900°C" PEALD polycrystalline alumina films were characterized by high dielectric constant ($\varepsilon_r = 10.1$) and lower fixed charge density ($N_{ss} = 3.6 \times 10^{12}$ cm^{-2}) (table 2). This confirms that a crystallization annealing at 900°C (or more) is required in order to improve the dielectric characteristics of Al_2O_3-based MIS capacitors.

3.3. Conduction properties of PEALD-Al₂O₃-based MIS capacitors

In order to decrease the impact of extrinsic defects on the dielectric breakdown, I-V analysis were performed on the smallest MIS capacitors (area: 1.6×10^{-6} cm^2) while considering the "as-deposited" and "annealed at 900°C" process conditions (figure 3). In both case, low current densities (200 nA/cm^2) were evidenced at low voltage (< 10 V). This current is associated to leakage as well as capacitive charging. Then, the current increase in the MIS structure occurs at approximately 11.5 V. Associated conduction phenomena were studied while considering two

different mechanisms: Fowler-Nordheim and Poole-Frenkel [21,23,25,36]. Whatever the process conditions used, the study of the I-V curves showed that the dominant mechanism is related to the Fowler-Nordheim conduction (figure 4), in agreement with previous results obtained for PEALD alumina films [21]:

$$J_{FN} = K_1 E^2 \ exp\left(-\frac{K_2}{E}\right)$$

(1)

where J_{FN} and E are the current density and the electric field into the insulative layer respectively, K_1 and K_2 being constant parameters, depending only on the studied dielectric material.

This implies that the conduction into amorphous and polycrystalline Al_2O_3 layer deposited by PEALD is related to the tunnel emission of trapped electrons towards the conduction band. Consequently, there is no electronic diffusion associated to defects in the bulk alumina.

Finally, breakdown occurs for applied voltage higher than 25 V, and breakdown properties of the $Al/Al_2O_3/Si$ MIS capacitors were studied finally for twenty different devices. Thus, as-deposited PEALD amorphous alumina films were characterized by lower breakdown electric field (E_{bd} = 8.4 ± 0.1 MV/cm) than "annealed" PEALD polycrystalline alumina ones (E_{bd} = 8.75 ± 0.1 MV/cm). Both results are excellent in the frame of "high-k" gate material for metal-oxide-silicon (MOS) microdevices but, as previously, the crystallization annealing at high temperature (900°C) is found to improve the conduction and breakdown properties of PEALD Al_2O_3 films.

3.4. pH detection properties of PEALD-Al_2O_3-based chemical field effect transistors

Whatever the characterization techniques chosen, i.e. I-V analysis using standard pH buffers (4.0, 7.0 and 10.0) or HCl/TMAH titration experiments, similar pH detection properties were obtained for the different PEALD-Al_2O_3-based ChemFET sensors, e.g. annealed or unannealed

(table 3). Nevertheless, results obtained with the second characterization techniques will only be presented because of their completeness on the [2 – 12] pH range.

Furthermore, in the frame of the pH-ChemFET process, the alumina film was deposited on a silicon dioxide layer rather on the silicon substrate. As a result, it was previously shown that the SiO_2/Al_2O_3 structure was characterized by steep interfaces and was therefore free from any major aluminosilicate Al_xSi_yO interfacial layer [12]. Consequently, bulk phenomena will only be considered in the following.

Concerning the unannealed SiO_2/Al_2O_3 pH-ChemFET (figure 5a) and as expected [37], excellent pH detection properties were evidenced (table 3), i.e. quasi-Nernstian response with no hysteresis phenomenon on the [2-12] pH range, low drift (< 1 mV/day) and long lifetime (> six months). In fact, compared to the standard SiO_2/Si_3N_4 pH-ChemFET, improvements related to alumina Al_2O_3 were associated to a higher sensitivity (59 mV/pH versus 55 mV/pH) as well as to lower sensitivities to potassium K^+ and sodium Na^+ ions in solution (1 mV/decade versus 15 mV/decade in the [1-3] pK or pNa range [38]). Such conclusions were of course expected, but the study of thermal annealing influences led finally to antagonist results (figures 5b to 5d). In fact, except for the drain-source leakage current under threshold which was slightly improved as part of device nominal operation, the annealing temperature increase was responsible for the global worsening, and finally the annihilation, of the pH detection properties PEALD-Al_2O_3-based pH-ChemFET (table 3). According to previous results [12], here is a way of clarifying such antagonist results according to an "Electrical Characterization" approach.

First of all, the 600°C anneal was responsible for a threshold voltage decrease (around 0.3-0.4 V) as well as for a positive hysteretic potential shift (around 0.2 V). Such variations should be related to a redistribution of electrical defects in the SiO_2/Al_2O_3 structure, leading to positive charge trapping into the pH-ChemFET dielectric layer. Since crystallisation cannot occur at temperature lower than 700°C [12], this phenomenon should be related to the preceding germination phase and

first related atomic rearrangements into the Al_2O_3 amorphous matrix. At 750°C, when alumina crystallization occurs effectively, the threshold voltage kept on decreasing (around 0.4-0.5 V more) while hysteresis remained unchanged. This tends to prove that charge trapping takes place at interfaces between the amorphous-Al_2O_3 phase and the polycrystalline-Al_2O_3 one. As a result, for the 800°C anneal, when alumina film crystallisation was completed and, consequently, the amorphous phase disappeared, pH detection properties similar to the initial unannealed one were finally obtained, evidencing quasi-Nernstian response with no hysteresis phenomenon on the [2-12] pH range (figure 5d).

Actually, the thermal annealing worsening was highlighted while considering temporal drifts and lifetimes obtained for the different PEALD-Al_2O_3-based pH-ChemFET devices. Indeed, the temperature increase was responsible for the temporal drift increase as well as to the lifetime collapse (table 3). For low temperature (600°C), since rearrangements into the Al_2O_3 matrix are minor, pH sensitivity remains quasi-Nernstian for long durations (at least 30 days) and low temporal drifts are still evidenced. Nevertheless, for higher temperatures (T > 700°C), if classical pH responses can be first obtained on a [2-12] pH range (figures 5c and especially 5d), PEALD-Al_2O_3-based pH-ChemFET showed rapidly high measurement instabilities (and therefore non-Nernstian sensitivities or even non-linear analytical responses) to pH. As a result, devices were no longer operational in water-based solutions after few days of use only.

Even if TMAH was found to be ineffective to etch the deposited PEALD-Al_2O_3 films and in order to tackle off its use during titration experiments, similar studies were conducted in different buffers (pH = 4.0, 7.0 and 10.0) with similar results. Doing so, it was shown that worsening phenomena were in fact related to the pH = 10 buffer and therefore to the use of alkaline solutions. Thus, specific drift experiments were performed on the 800°C-annealed SiO_2/Al_2O_3 pH-ChemFET (figure 6). For a neutral solution (pH ≈ 7.2), an initial output voltage around 50 mV was found on a 10-hour period, in agreement with previous temporal drift result if such a low duration is

considered. On the contrary, important potential instabilities related to strong leakage currents were evidenced for an alkaline solution (pH $\approx$ 11.4). After such treatment, it appears that the studied PEALD-Al$_2$O$_3$-based pH-ChemFET is still operational for a while, being definitively deteriorated after repeated experiments. Actually, this effect should be related to a physico-chemical degradation of the SiO$_2$/Al$_2$O$_3$ insulative layer during the crystallization anneal at high temperature (T $\geq$ 700°C). Since a polycrystalline-Al$_2$O$_3$ matrix was finally obtained, it is assumed that hydroxide OH$^-$ ion diffusion or/and electromigration take place in the newly-created grain boundaries passing through the alumina dielectric film, being finally responsible for leakage currents and lethal water-based dielectric breakdown when immersed in solutions.

So, if detection and insulation/passivation materials for potentiometric pH-ChemFET-based microsensors are considered, the best dielectric properties were finally obtained for the as-deposited, unannealed, amorphous PEALD-Al$_2$O$_3$-based films.

4. Conclusion

In summary, Al$_2$O$_3$ films were deposited on silicon substrates by plasma-enhanced atomic layer deposition (PEALD) using TMA/O$_2$ precursors, and their dielectric/passivation properties were analysed while focusing on the influences of thermal annealing under a dioxygen O$_2$ ambient. In this context, antagonist results were evidenced.

On the one hand, dealing with high-k gate materials for metal-oxide-silicon (MOS) microdevices, the dielectric properties of PEALD-Al$_2$O$_3$-based films are optimized for polycrystalline alumina films and, therefore, are improved by a crystallization annealing performed at high temperature (T > 700°C). So, the best properties were obtained for a 900°C anneal, evidencing low fixed charge density (4×10^{12} cm^{-2}), high dielectric constant ($\varepsilon_r \approx 10.2$), Fowler-Nordheim tunnelling conduction and high breakdown electric fields (E$_{bd} \approx 8.75$ MV/cm).

On the other hand, focusing on detection/passivation insulative materials for potentiometric microsensors in water-based solutions, alumina crystallization was found to be responsible for prohibitive drawbacks. Indeed, even if quasi-Nernstian pH responses were first evidenced in a [2-12] pH range, high temperature anneals (T > 700 °C) were associated to leakage currents, high temporal drifts and low lifetimes in watery phase (especially in alkaline solutions, pH > 7), being finally responsible for the annihilation of the pH-sensitive/insulative properties of the PEALD Al_2O_3 films. So, in this case, such properties are optimized for as-deposited, unannealed, amorphous alumina films.

These investigations allow to have a better understanding of the influence of thermal annealing on the properties of PEALD-Al_2O_3-based films. They will be helpful for further micro/nano-technological applications, and especially for the integration and the passivation of silicon-nanowire-based, pH-sensitive, chemical field effect transistors for the liquid phase analysis at the nanoscale.

References

[1]   P. Nayar, A. Khanna, D. Kabiraj, S.R. Abhilash, B.D. Beake, Y. Losset and B. Chen, "Structural, optical and mechanical properties of amorphous and crystalline alumina thin films", Thin Solid Films, 568 (2014) 19-24

[2]   P.J. Kelly and R.D. Arnell, "Control of the structure and properties of aluminium oxide coating by pulsed magnetron sputtering", Journal of Vacuum Science and Technology, A17 (1999) 945-953

[3]   C. Hibert, H. Hidalgo, C. Champeaux, P. Tristant, C. Tixier, J. Desmaison and A. Catherinot, "Properties of aluminium oxide thin films deposited by pulsed laser deposition and plasma enhanced chemical vapour deposition", Thin Solid Films, 516 (2008) 1290-1296

[4]   S. Ruppi, "Deposition, microstructure and properties of texture-controlled CVD α-Al_2O_3 coatings", International Journal of Refractory Metals and Hard Materials, 23 (2005) 306-316

[5]   Q.Y. Shao, A.D. Li, H.Q. Ling, D. Wu, Y. Wang, Y. Feng, S.Z. Yang, Z.G. Liu, M. Wang and N.B. Ming, "Growth and characterization of Al_2O_3 gate dielectric films by low-pressure metalorganic chemical vapor deposition", Microelectronic engineering, 66 (2003) 842-848

[6]   R.S. Johnson, G. Lucovski and I. Baumvol, "Physical and electrical properties of nanocrystalline prepared by remote plasma enhanced chemical vapour deposition", Journal of Vacuum Science and Technology, A19 (2001) 1353-1360

[7]   S.C. Ha, E. Choi, S.H. Kim and J.S. Roh, "Influence of oxidant source on the property of atomic layer deposited Al_2O_3 on hydrogen-terminated Si substrate", Thin Solid Films, 476 (2005) 252-257

[8]   J.L. Van Hemmen, S.B.S. Heil, J.H. Klootwijk, F. Roozeboom, C.J. Hodson, M.C.M. van de Sanden and W.M.M. Kessels, "Plasma and thermal ALD of Al_2O_3 in a commercial 200 mm ALD reactor", Journal of the Electrochemical Society, 154 (2007) G165-G169

[9]   V.R. Rai, V. Vandalon and S. Agarwal, "Influence of surface temperature on the mechanism of atomic layer deposition of aluminium oxide using an oxygen plasma and ozone", Langmuir, 28 (2012) 350-357

[10]   S.E. Potts, H.B. Profikt, R. Roelofs and W.M.M. Kessels, "Room-temperature ALD of metal oxide thin films by energy-enhanced ALD", Chemical Vapor Deposition, 19 (2013) 125-133

[11]   L. Aarik, T. Arroval, R. Rammula, H. Mändar, V. Sammelselg, B. Hudec, K. Husekova, K. Fröhlich and J. Aarik, "Atomic layer deposition of high-quality Al_2O_3 and Al-doped TiO_2 thin films from hydrogen-free precursors", Thin Solid Films, 565 (2014) 19-24

[12] A. Lale, E. Scheid, F. Cristiano, L. Datas, B. Reig, J. Launay and P. Temple-Boyer: "Study of aluminium oxide thin films deposited by plasma-enhanced atomic layer deposition from tri-methyl-aluminium and dioxygen precursors: investigation of interfacial and structural properties", Thin Solid Films, 666 (2018) 20-27

[13] R.M. Wallace and G.D. Wilk, "High-k dielectric materials for microelectronics", Critical Reviews in Solid State and Materials Sciences, 28 (2003) 231-285

[14] J.A. Kittl, K. Opsomer, M. Popovici, N. Menou, B. Kaczer, X.P. Wang, C. Adelmann, M.A. Pawlak, K. Tomida, A. Rothschild, B. Govoreanu, R. Degraeve, M. Schaekers, M. Zahid, A. Delabie, J. Meersschaut, W. Polspoel, S. Clima, G. Pourtois, W. Knaepen, C. Detavernier, V.V. Afanas'ev, T. Blomberg, D. Pierreux, J. Swerts, P. Fischer, J.W. Maes, D. Manger, W. Vandervorst, T. Conard, A. Franquet, P. Favia, H. Bender, B. Brijs, S. Van Elshocht, M. Jurczak, J. Van Houdt and D.J. Wouters, "high-k dielectrics for future generation memory devices", Microelectronic Engineering, 86 (2009) 1789-1795

[15] O. Knopfmacher, A. Tarasov, W. Fu, M. Wipf, B. Niesen, M. Calame and C. Schönenberger, "Nernst limit in dual-gated Si-nanowire FET sensors", Nanoletters, 10 (2010) 2268-2274

[16] S. Chen, J.G. Bomer, E.T. Carlen and A. van den Berg, "Al_2O_3/silicon nanoISFET with near ideal Nernstian response", Nanoletters, 11 (2011) 2334-2341

[17] B. Reddy, B.R. Dorvel, J. Go, P.R. Nair, O.H. Elibol, G.M. Credo, J.S. Daniels, E.K.C. Chow, X. Su, M. Varma, M.A. Alam, and R. Bashir, "High-k dielectrics Al_2O_3 nanowire and nanohotplate field effect sensors for improved pH sensing", Biomedical Microdevices, 13 (2011) 335-344

[18] K. Bedner, V.A. Guzenko, A. Tarasov, M. Wipf, R.L. Stoop, D. Just, S. Rigante, W. Fu, R.A. Minamisawa, C. David, M. Calame, J. Gobrecht and C. Schönenberger, "pH response of silicon nanowire sensors: impact response of nanowire width and gate oxide", Sensors and Materials, 25 (2013) 567-576

[19] L. Wang, L. Li, T. Zhang, X. Liu and J.-P. Ao, "Enhanced pH sensitivity of AlGaN/GaN ion-sensitive field effect transistor with Al_2O_3 synthetized by atomic layer deposition", Applied Surface Science, 427 (2018) 1199-1202

[20] S. Rollo, D. Rani, W. Olthuis and C.P. Garcia, "High performance Fin-FET electrochemical sensor with high-k dielectric materials", Sensors and Actuators, B303 (2020) 127215 1-7

[21] K.B. Jinesh, J.L. van Hemmen, M.C.M. van de Sanden, F. Roozeboom, J.H. Klootwijk, W.F.A., Besling and W.M.M. Kessels, "Dielectric properties of thermal and plasma-assisted atomic layer deposition Al_2O_3 thin films", Journal of the Electrochemical Society, 158 (2011), G21-G26

[22] M.D. Groner, J.W. Elam, F.H. Fabreguette and S.M. George, "Electrical characterization of thin Al_2O_3 films grown by atomic layer deposition on silicon and various metal substrates", Thin Solid Films, 413 (2002) 186-197

[23] C. Lin, J. Kang, D. Han, D. Tian, W. Wang, J. Zhang, M. Liu, X. Liu and R. Han, "Electrical properties of Al_2O_3 gate dielectrics", Microelectronic Engineering, 66 (2003) 830-834

[24] J. Buckley, B. De Salvo, D. Deleruyelle M. Gely, G. Nicotra, S. Lombardo, J.F. Damlencourt, P. Hollinger, F. Martin and S. Deleonibus, "Reduction of fixed charges in atomic layer deposited Al_2O_3 dielectrics", Microelectronic Engineering, 80 (2005) 210-213

[25] B. Han, S.W. Lee, K. Park, C.O. Park, S.K. Rha and W.J. Lee, "The electrical properties of dielectric stacks of SiO_2 and Al_2O_3 prepared by atomic layer deposition methods", Current Applied Physics, 12 (2012) 434-436

[26] D.J. Lee, J.W. Lim, J.K. Mun and S.J. Yun, "Improved stability of electrical properties of nitrogen-added Al_2O_3 films grown by PEALD as gate dielectrics", Materials Research Bulletin, 83 (2016) 597-602

[27] M. Shukla, G. Dutta, R. Mannam and N. Dasgupta, "Electrical properties of reactive-ion sputtered Al_2O_3 on 4H-SiC", Thin Solid Films, 607 (2016) 1-6

[28] S. Hlali, N. Hizem, L. Militaru, A. Kalboussi and A. Souifi, "Effect of interface traps for ultra-thin high-k gate dielectric based MIS devices on the capacitance-voltage characteristics", Microelectronics reliability, 75 (2017) 154-161

[29] L. Bousse, H.H. van den Vlekkert and N.F. de Rooij, "Hysteresis effect in Al_2O_3 gate ISFETs", Sensors and Actuators, B2 (1990) 103-110

[30] J.C. Chou and. C-Y. Weng, "Sensitivity and hysteresis effect in Al2O3 gate pH-ISFET", Materials Chemistry and Physics, 71 (2001) 120-124

[31] L. Manjakal, D. Szwagierczak and R. Dayiya, "Metal oxides based electrochemical pH sensors: current progress and future perspectives", Progress in Materials Science, 109 (2020) 100635 1-31

[32] S.C. Ha, E. Choi, S.H. Kim and J.S. Roh, "Influence of oxidant source on the property of atomic layer deposited Al_2O_3 on hydrogen-terminated Si substrate", Thin Solid Films, 476 (2005) 252-257

[33] S.M. Sze, "Physics of semiconductors devices, 2nd edition, chapter 7: MIS diode and charge-coupled devices", John Wiley & Sons Inc., Canada (1981)

[34] P. Temple-Boyer, J. Launay, I. Humenyuk, T. Do Conto, A. Martinez, C. Bériet and A. Grisel: "Study of front-side connected chemical field effect transistors for water analysis ", Microelectronics Reliability, 44 (2004) 443-447

[35] "Metals, Alloys, Compounds, Ceramics, Polymers, Composites, catalogue 1993/1994", Goodfellow Metals Limited, Cambridge, United Kingdom (1993)

[36] B. Hajji, P. Temple-Boyer, F. Olivié, A. Martinez, "Electrical characterization of thin silicon oxynitride films deposited by low pressure chemical vapour deposition", Thin Solid Films, 354 (1999) 9-12

[37] P. Bergveld, "Thirsty years of ISFETOLOGY: what happen in the last 30 years and what may happen in the next 30 years, Sensors and Actuators, B88 (2003) 1-20

[38] B. Hajji, P. Temple-Boyer, J. Launay, T. Do Conto, A. Martinez, "pH, pK and pNa detection properties of SiO_2/Si_3N_4 ISFET chemical sensors", Microelectronics Reliability, 40 (2000) 783-786

Tables and figures captions

Table 1: C-V analysis of a 400-cycle TMA/O_2 PEALD Al_2O_3 films

annealed 5 minutes under an O_2 gaseous atmosphere at different temperatures

Table 2: C-V analysis of Al/Al_2O_3/Si MIS capacitors (number of PEALD cycles: 325)

for two process conditions: "as-deposited" and "annealed at 900°C"

Table 3: pH detection properties of SiO_2/Al_2O_3 ChemFET sensors

annealed 5 minutes under an O_2 ambient at different temperatures

Figure 1: C-V curves of PEALD-Al_2O_3/Si structure (PEALD cycle number: 400)

a) as-deposited, b) annealed 5 minutes under an O_2 ambient at 850°C

Figure 2: C-V curves of PEALD-Al_2O_3 MIS capacitors (PEALD cycle number: 325)

a) as-deposited, b) annealed 5 minutes under an O_2 ambient at 900°C

Figure 3: I-V curves of PEALD-Al_2O_3 MIS capacitors (PEALD cycle number: 325)

a) as-deposited, b) annealed 5 minutes under an O_2 ambient at 900°C

Figure 4: Fowler-Nordheim characteristics of PEALD-Al_2O_3 MIS capacitors (cycle number: 325)

a) as-deposited, b) annealed 5 minutes under an O_2 ambient at 900°C

Figure 5: pH detection properties of SiO$_2$/Al$_2$O$_3$ ChemFET

a) unnealed (as-deposited), b) annealed 5 minutes under O$_2$ at 600°C,

c) annealed 5 minutes under O$_2$ at 750°C, d) annealed 5 minutes under O$_2$ at 800°C

Figure 6: temporal drift of the 800°C-annealed SiO$_2$/Al$_2$O$_3$ pH-ChemFET

in neutral (pH ≈ 7.2) and alkaline (pH ≈ 11.4) solutions

annealing temperature (O$_2$ ambient, 5 minutes)	no anneal (as-deposited)	650°C	750°C	850°C	900°C	950°C	1000°C
Al$_2$O$_3$ thickness (nm)	37.5 nm	37 nm	34.5	33	32	31	31
SiO$_2$ thickness (nm)	-	-	2	2.5	3	4	4.5
total thickness (nm)	37.5	37	36.5	35.5	35	35	35.5
flat-band voltage (V)	7.5	4.5	4.5	3.4	2.5	2.2	2.7
capacitance in accumulation (pF)	850	840	840	950	950	920	890
Al$_2$O$_3$ dielectric constant	8.6	8.4	8.8	10.1	10.2	10.2	10.2
fixed charge density ($\times 10^{12}$ cm^{-2})	10.0	6.1	6.1	5.2	4.1	3.6	4.1

Table 1: C-V analysis of a 400-cycle TMA/O$_2$ PEALD Al$_2$O$_3$ films

annealed 5 minutes under an O$_2$ ambient at different temperatures

Process conditions	no anneal (as-deposited)	annealed 5 minutes at 900°C, O_2 ambient
Al_2O_3 thickness (nm)	30	27.5
SiO_2 thickness (nm)	-	3
total thickness (nm)	30	30.5
flat-band voltage (V)	4.6	2.6
capacitance in accumulation (nF)	19.6	20.0
Al_2O_3 dielectric constant	8.5	10.1
fixed charge density ($\times 10^{12}$ cm^{-2})	6.6	3.5

Table 2: C-V analysis of Al/Al_2O_3/Si MIS capacitors (number of PEALD cycles: 325)

for two process conditions: "as-deposited" and "annealed at 900°C"

annealing temperature (O$_2$ ambient, 5 minutes)	no anneal	600°C anneal	750°C anneal	800°C anneal
Gate-source voltage at pH = 7 (V)	1.80 ± 0.05	1.45 ± 0.05	1.00 ± 0.05	1.70 ± 0.05
drain-source leakage current (μA)	~ 8.5	~ 4	~ 4.5	~ 1
hysteresis potential shift (V)	$- 0.02 \pm 0.05$	0.20 ± 0.05	0.15 ± 0.05	$- 0.05 \pm 0.05$
pH sensitivity (mV/pH)	~ 59	~ 58	~ 57	~ 57
lifetime (day)	> 180	> 30	6	5
temporal drift at pH = 7 (mV/day)	< 1	~ 10	~ 30	~ 40

Table 3: pH detection properties of SiO$_2$/Al$_2$O$_3$ ChemFET sensors

annealed 5 minutes under an O$_2$ ambient at different temperatures
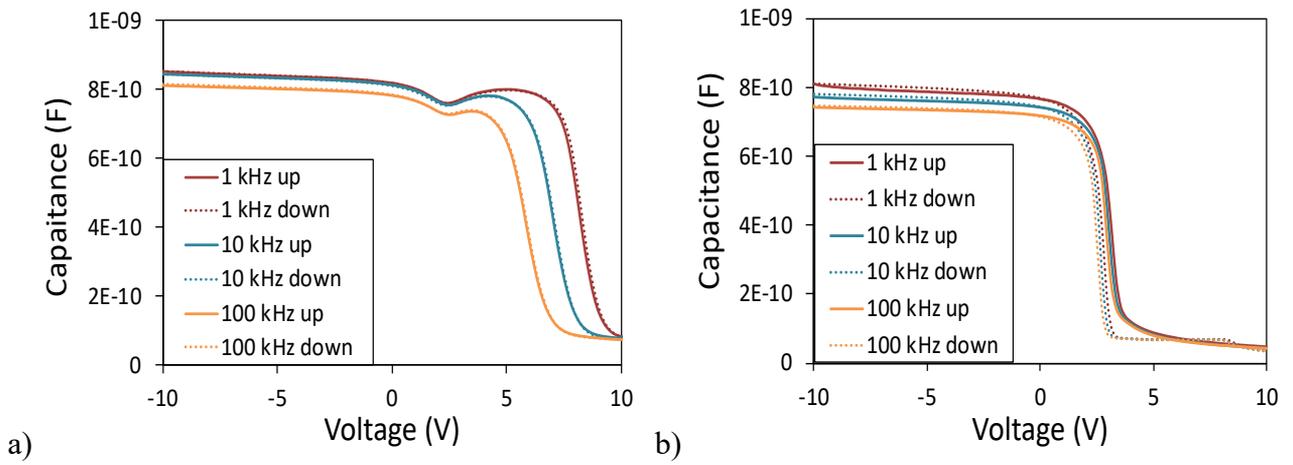
Figure 1: C-V curves of PEALD-Al$_2$O$_3$/Si structure (PEALD cycle number: 400)

performed using a mercury probe with a 4.18×10^{-3} cm^2 contact area

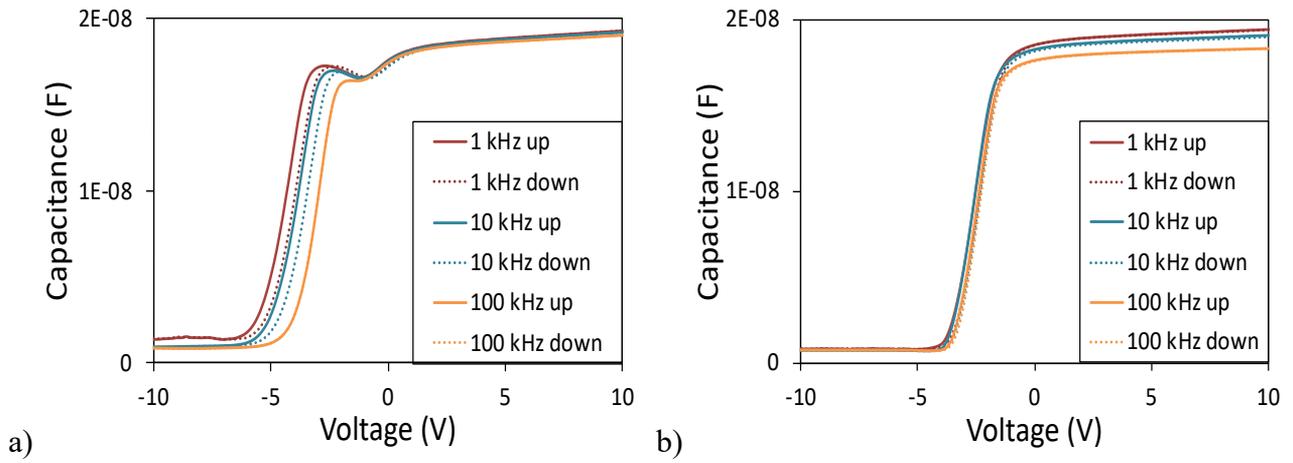a) as-deposited, b) annealed 5 minutes under an O$_2$ ambient at 850°C

a)

b)

Figure 2: C-V curves of PEALD-Al_2O_3 MIS capacitors (PEALD cycle number: 325)

performed using a MIS capacitor with a 7.84×10^{-2} cm^2 area

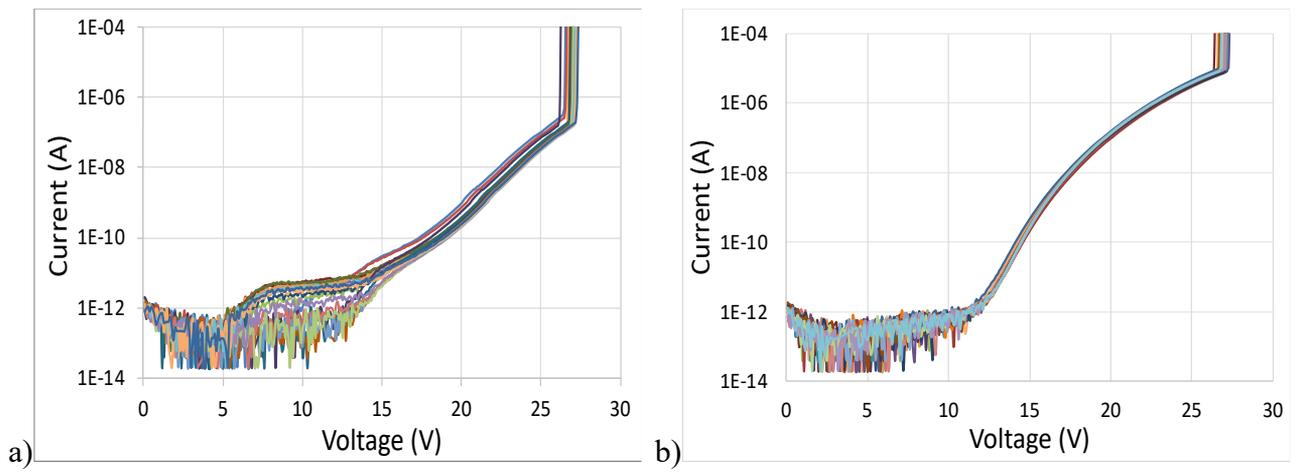a) as-deposited, b) annealed 5 minutes under an O_2 ambient at 900°C

Figure 3: I-V curves of PEALD-Al$_2$O$_3$ MIS capacitors (PEALD cycle number: 325)

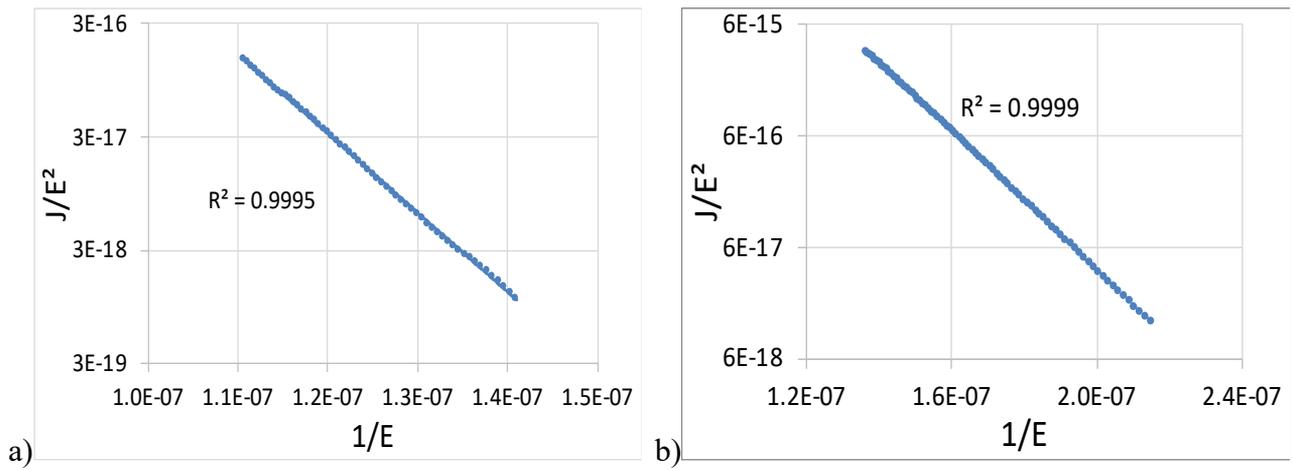a) as-deposited, b) annealed 5 minutes under an O$_2$ ambient at 900°C

Figure 4: Fowler-Nordheim characteristics of PEALD-Al_2O_3 MIS capacitors (cycle number: 325)

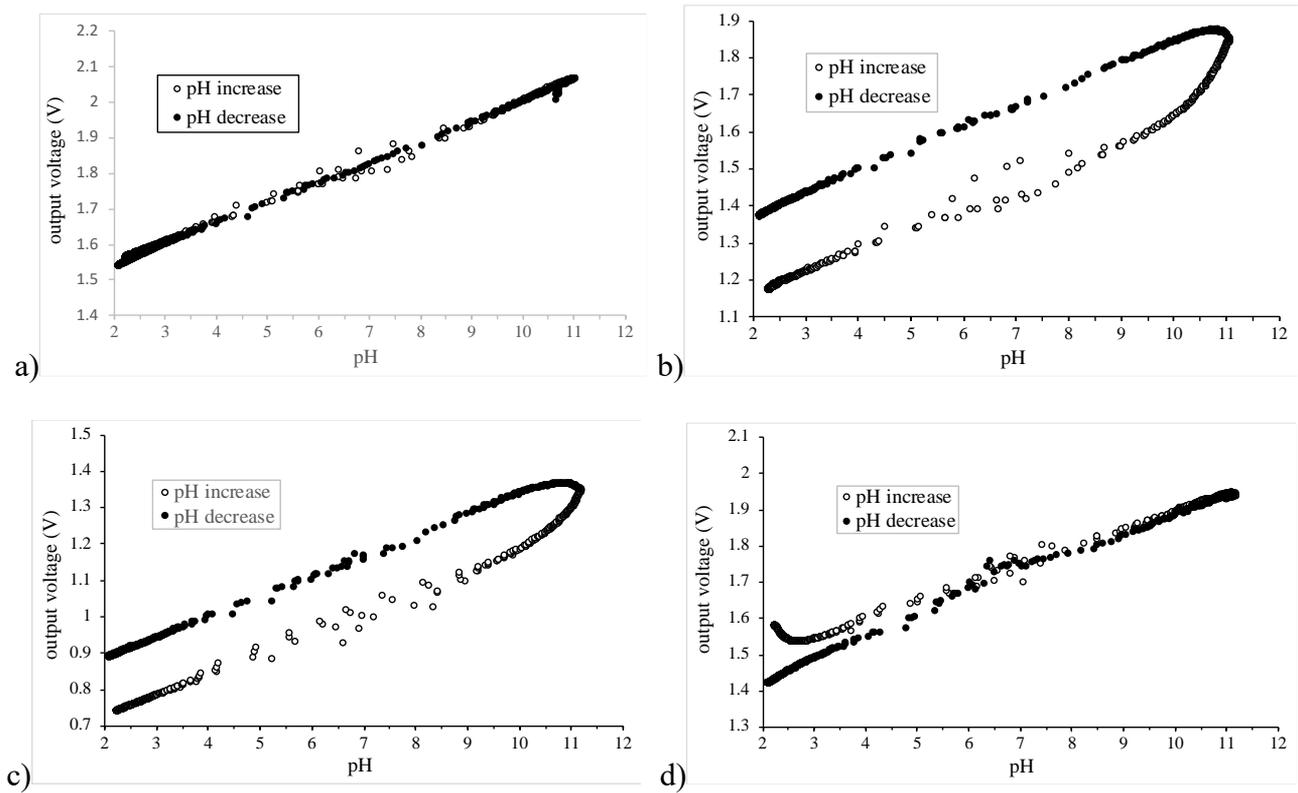a) as-deposited, b) annealed 5 minutes under an O_2 ambient at 900°C

Figure 5: pH detection properties of SiO$_2$/Al$_2$O$_3$ ChemFET

a) unnealed (as-deposited), b) annealed 5 minutes under O$_2$ at 600°C,

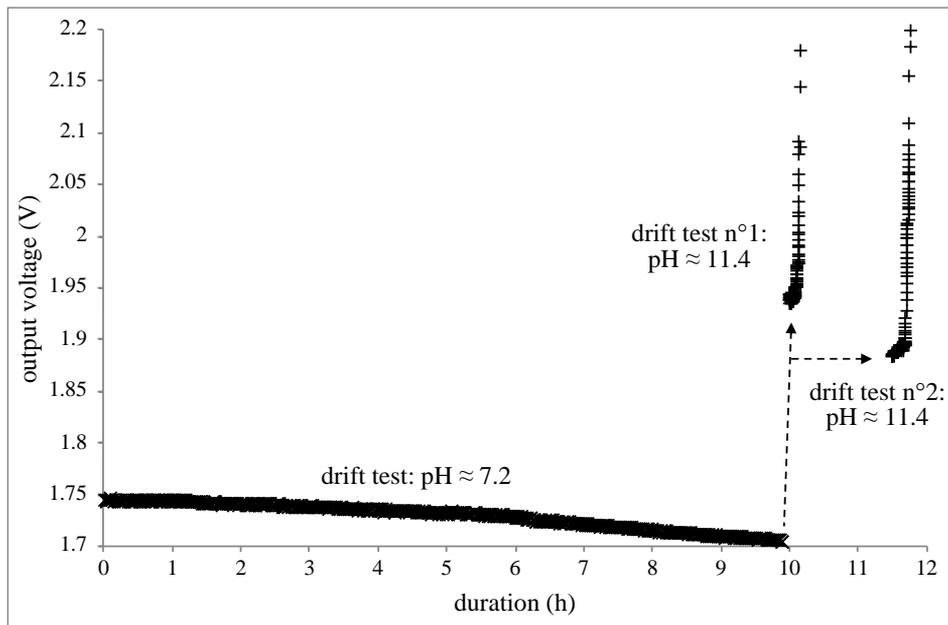c) annealed 5 minutes under O$_2$ at 750°C, d) annealed 5 minutes under O$_2$ at 800°C

Figure 6: temporal drift of the 800°C-annealed SiO_2/Al_2O_3 pH-ChemFET

in neutral (pH ≈ 7.2) and alkaline (pH ≈ 11.4) solutions